HHS Public Access

Author manuscript

Neuroimage. Author manuscript; available in PMC 2016 August 01.

Published in final edited form as:

Neuroimage. 2015 August 1; 116: 222–231. doi:10.1016/j.neuroimage.2015.04.003.

Arousal Transitions in Sleep, Wakefulness, and Anesthesia are Characterized by an Orderly Sequence of Cortical Events

Xiao Liu[1,*], **Toru Yanagawa**[2], **David A. Leopold**[3], **Catie Chang**[1], **Hiroaki Ishida**[4], **Naotaka Fujii**[2], and **Jeff H. Duyn**[1]

[1]Advanced MRI Section, Laboratory of Functional and Molecular Imaging, National Institute of Neurological Disorders and Stroke, National Institutes of Health, Bethesda, MD, USA

[2]Laboratory for Adaptive Intelligence, Brain Science Institute, RIKEN, Saitama, Japan

[3]Section on Cognitive Neurophysiology and Imaging, Laboratory of Neuropsychology, National Institute of Mental Health, National Institutes of Health, Bethesda, MD, USA; Neurophysiology Imaging Facility, National Institute of Mental Health, National Institute of Neurological Disorders and Stroke, National Eye Institute, Bethesda, MD 20892

[4]Frontal Lobe Function Project, Tokyo Metropolitan Institute of Medical Science, Tokyo, Japan

Abstract

Many aspects of brain function are influenced by modulatory processes, including arousal. The most abrupt changes in arousal occur at the wake-sleep transition and at the induction of anesthetic conditions. They are accompanied by major electrophysiological changes, including an emergence of low-frequency (sleep-like) activity and a loss of mid-frequency (wake-like) activity that has been linked to feedback processes of the brain. Nevertheless, the causal relationship between these two types of electrophysiological changes, as well as the cortical mechanisms underlying changes in arousal and consciousness, remain poorly understood. To address this, we studied spontaneous electro-cortical activity during arousal changes in macaques. During sleep and at loss of consciousness induced by propofol anesthesia, we identified a prototypical sequence of cortical events in which the loss of mid-frequency activity preceded, by seconds, the increases in low-frequency activity. Furthermore, in visual areas, an influence of mid-frequency change onto high-frequency activity was observed across visual hierarchy. These results are consistent with the notion that drops in arousal and consciousness are facilitated by a release of feedback cortical inhibition.

[*]Corresponding Author: Xiao Liu, PhD, 10 Center Dr., Bldg. 10, Rm. B1D-723A - MSC 1065, Bethesda, MD 20892-1065, USA, Tel.: +1 301 594 7312, Fax: +1 301 480 1981, liux15@ninds.nih.gov.

Contributions

X.L. and J.H.D designed the study and performed the analysis; T.Y., H.I., and N.F. acquired the data; X.L., D.A.L., C.C., and J.H.D wrote the paper.

Competing financial interests

The authors declare no competing financial interests.

Keywords

Resting-state global signal; Consciousness; Feedback Process; Alpha Inhibitory Gating; Sleep; Propofol Anesthesia

Introduction

Our ability to perceive environmental stimuli and perform cognitive tasks is influenced by the arousal level of the brain, which varies substantially across the day. The most dramatic and abrupt changes occur during the transition into sleep or anesthetic states, where entry into unconsciousness is accompanied by strong, widespread electrophysiological changes. Typically, these changes are characterized by a decrease in mid- to high-frequency (> 8 Hz) activity and an increase in low-frequency (< 4 Hz) activity (Davis et al., 1937; Magoun, 1952; Steriade, 2006).

Despite these clear electrophysiological changes, the mechanistic understanding of changes in perception and cognition with fading arousal and loss of consciousness (LOC) remains incomplete. Consistent with these spectral changes, brain activity at the middle frequency range (8–30 Hz) activity has been linked to top-down, feedback control of sensory input processing (Buschman and Miller, 2007; van Kerkoerle et al., 2014; von Stein et al., 2000), which is a feature of consciousness. Indeed, there is evidence that feedback information flow may be reduced under conditions of reduced consciousness (Boly et al., 2012; Imas et al., 2005; Jordan et al., 2013; Ku et al., 2011; Lee et al., 2013; Yanagawa et al., 2013). Nevertheless, little is known about how these feedback processes are disrupted at the time LOC occurs. One possibility is that the low frequency activity typical of sleep/anesthesia impedes the effectiveness of mid- to high-frequency activity in transferring information between distant cortical regions. For example, the UP and DOWN states associated with slow oscillations (< 1Hz) may occur asynchronously in these distant regions, impeding effective neuronal signaling (Lewis et al., 2012). Alternatively, or additionally, information transfer (and processing) may be impeded by the restricted repertoire of neuronal spiking patterns afforded by the UP and DOWN states (Alkire et al., 2008).

However, an interesting, alternative possibility is that a reduction in feedback activity facilitates, and therefore precedes, the emergence of slow oscillations. This hypothesis is inspired by studies of the interaction between wake- and sleep-promoting neurons at the forebrain and brainstem. These two groups of neurons, possibly in concert with cortical units (Steenland, 2014), have been found to jointly orchestrate lapses in arousal and consciousness. Specifically, activity changes in one group are thought to disturb the delicate balance of mutual inhibition between two groups and lead to an abrupt arousal transition and widespread cortical activity (Saper et al., 2010; Saper et al., 2005). Interestingly, investigations of the interaction between these two groups of subcortical neurons in mice at the wake-sleep transition have found a reproducible order of events, in which an initial firing rate decrease of wake-promoting neurons preceded, by about one second, the increased firing of sleep-promoting neurons (Takahashi et al., 2010; Takahashi et al., 2009). This order of events is consistent with the notion that a reduction in cortical feedback activity

precedes the emergence of slow oscillations. Given the strong influence of subcortical wake- and sleep-promoting systems on cortical activity (Moruzzi and Magoun, 1949), and the potential for the reverse interaction (Steenland, 2014), the sequence of subcortical events leading up to LOC could be accompanied by corresponding changes in the cortex. Thus, monitoring cortical dynamics at arousal transitions may reveal evidence for dissociated changes in wake- and sleep-related neural processes and thus inform on the mechanisms underlying LOC.

To investigate this possibility, we recorded spontaneous electro-cortical activity in non-human primates across a range of behavioral states, including sleep. We focused on micro-arousal changes associated with cyclic alternating patterns (CAP) of sleep (Halasz et al., 2004; Terzano and Parrino, 2000), as well as large arousal drops at the induction of propofol anesthesia. By investigating temporal changes in spectral characteristics of the electrophysiological signals, we were able to associate arousal drops with a prototypical pattern of sequential activity changes in distinct frequency bands. The initiating event in this pattern was a drop in mid-frequency power, which has previously been linked to feedback activity(Buschman and Miller, 2007; van Kerkoerle et al., 2014; von Stein et al., 2000; Yanagawa et al., 2013).

Methods

Subjects and materials

Electrocorticography (ECoG) signals were recorded from 4 macaque monkeys whose brains had been chronically implanted with customized 128-channel electrode arrays (Unique Medical, Japan) (Nagasaka et al., 2011) covering an extensive portion of the cortical surface of a single (left) hemisphere (for example, see Fig 1a). The electrodes consisted of 3 mm diameter platinum discs that were insulated with a layer of silicone except for a small (0.8 mm diameter) disc-shaped area at the center. The array was implanted subdurally in 4 adult macaque monkeys (monkeys C, G, K are Macaca fuscata, and monkey S is Macaca mulatta), covering a contiguous area that included the frontal, parietal, temporal, occipital lobes of the left hemisphere. A reference electrode consisting of a rectangular platinum plate was placed in the subdural space between the ECoG array and dura mater, and a ground electrode was placed in the epidural space (See (Nagasaka et al., 2011) for detailed descriptions). The position of ECoG electrodes in monkeys C, K and S was manually remapped onto the brain of monkey G. ECoG signals were recorded at a sampling rate of 1 kHz using a Cerebus data acquisition system (Blackrock, UT, USA). Electrooculography (EOG) and electromyography (EMG) signals were also recorded at a sampling rate of 1 kHz using the same acquisition system. The EOG signal was recorded from muscles of the right eye in the horizontal direction. Two electrodes (Nihon Kohden, Disposable electrode for ECG Monitoring M-150) were put on the tail and the inner corner of right eye respectively and the potential difference between them was used as EOG signal. Another two electrodes were put on the chin and their potential difference was used as EMG signal.

All experimental and surgical procedures were performed in accordance with the experimental protocols (No. H24-2-203(4)) approved by the RIKEN ethics committee and the recommendations of the Weatherall report “The use of non-human primates in research”.

Experimental procedures

Conditions of natural sleep (monkeys C,G), propofol anesthesia (C,G), and rest with eyes-open (EO) and eyes-closed (EC) (C,G,K,S) were studied. Recordings during sleep were performed in 2 monkeys (C and G) over 6 experiments with a total recording time of ~7.2 hours. Spontaneous activity under the EO and EC conditions was recorded for all 4 monkeys in 21 experiments over a total period of ~10 hours. Propofol anesthetic, which is thought to take effect by potentiating $GABA_A$ ion channels, was given to 2 monkeys (C and G) through an intravenous injection (~5.2 mg/kg), and ECoG signals were monitored throughout the experiments.

All 21 experiments included rest eyes-closed (EC) and eyes-open (EO) conditions. Under the EC condition, monkeys were calmly seated in a dedicated chair with arms and head movement restricted and eyes covered with a mask. Under the EO condition, the eye mask was removed and the monkeys kept their eyes open. The recording under the EC and EO conditions lasted 10 to 20 minutes in each experiment and a total of ~10 hours in all experiments. We only used the data of EC sessions in 11 experiments, because there were some external perturbations in the other 10 experiments.

To facilitate the study of sleep, monkeys (C and G) were sleep deprived during the night before the experiment. Compared with the EC session recordings, we minimized environmental interferences by turning off the lights and keeping the room quiet. As a result, strong slow wave activity started to appear, in all 6 sessions, after the monkeys were left in the room for a few minutes. We then recorded the signals for a period of time (~ up to 1.5 hours for each session, and 7.2 hours in total for all 6 experiments) much longer than the EC sessions, and the conspicuous slow wave activity was consistently seen, though appearing intermittently, throughout the recordings.

In 4 experiments on monkeys C and G, after the EC and EO acquisitions, we started to monitor heart rate and then inject propofol (5.2 mg/kg) intravenously. We focused only on the induction period around the time of injection in this study. While the arousal level of monkeys was not behaviorally measured at the induction period, the heart rate, EOG, and EMG signals all showed a sudden drop, associated with a change in ECoG, about half a minute after the bolus injection of propofol. This likely indicate a suppression of arousal, given the fast action of propofol.

ECoG signals were also recorded during a food-reaching task in additional 3 experiments in the monkeys C. During the experiments, an experimenter was sitting in front of monkey with a table between them. There were multiple tasks in the experiments, but we only used data from the food-reaching trials. During each of these 290 trials, another experimenter put foods (a piece of apple) in front of both the monkey and the first experimenter, and the monkey reached for the food and ate it. The onset time of the monkey's hand movement was recorded for each trial, and their average interval is 33.65±37.07 seconds (range: 8.38-349.00 seconds).

Global mean spectrograms

Raw ECoG signals were first visually inspected for artifacts. Some experiments showed serious line-noise contamination, and these channels were excluded from further analysis (0, 2, 1, and 1 out of 128 channels for monkeys C, G, K, and S, respectively). Line noise and its harmonics were then removed using a sine wave fitting method provided by Chronux, a matlab package for the analysis of neural data (Mitra and Bokil, 2008). Individual channels were also re-referenced to the common mean of all the channels. After that, we applied a multi-taper time-frequency transformation (Thomson, 1982) (1 second window, 0.2 second sliding step, and 5 tapers) to each channel using Chronux functions, which generated spectrograms showing temporal evolution of ECoG powers at each 1-Hz frequency bin between 1-100Hz. The power was further converted into decibel (dB) units with a logarithmic operation. For each frequency bin, the temporal mean of spectral power was then subtracted out. This mean subtraction step served to equalize spectral power of the ECoG signal at different frequencies (often following an ~1/f dependence) and to make the subsequent analysis focus only on deviations from the baseline (temporal mean). For the propofol experiments, the mean subtraction procedure was made with reference to the period before the injection, because the baseline powers change dramatically after the propofol injection. The mean-subtracted spectrograms were then averaged over channels to give a global mean spectrogram.

Band-limited powers (BLPs)

The analysis of this study focused on the relative timing of aggregate neuro-electrical activity in three specific spectral frequency bands: the low-frequency (delta) band (<4 Hz), the mid-frequency (alpha-beta) band (9-21 Hz), and the high-frequency (broadband gamma) band (42-87 Hz). The precise boundaries of these frequency bands were chosen based on initial inspection of the time-frequency spectrogram (Fig 1c). The mean-subtracted spectrogram of individual channels was averaged across frequencies within the three bands to generate corresponding band-limited powers (BLPs). The BLPs were then used for computing spatial synchronization index (SSI) for each frequency band, as well as the cross-correlation functions between frequency bands.

SSI was calculated as the fraction of channels whose BLPs, at any specific time, show deviations larger than 1 standard deviation (SD). As the mid-frequency BLP showed modulation opposite to those at the low- and high-frequency bands, the “deviation” means “increase” for the low- and high-frequency bands, but “reduction” for the mid-frequency band. Cross-correlation (Pearson’s correlation) functions were calculated between the mid- and low-frequency BLPs and between the mid- and high-frequency BLPs with time lags range from −20 s to 20 s. To balance the degrees of freedom, this analysis was done on 300-sec sessions instead of the continuous data and the results were then averaged.

Event-triggered averaging

To obtain an average pattern of the sequential spectral transition (SST) events (see Results), we detected time points where the high-voltage low-frequency activity emerges across a widespread area. This is because these time points are around the middle of the SST patterns, and associated with sharp changes in both the low- and mid-frequency SSIs. They

were defined as threshold-crossing points (only those at the rising phase) of the low-frequency SSI at a threshold of 0.4, representing the time points where more than 40% channels started to show high (1 SD above average) low-frequency activity. Any detected time point with another one preceding it by less than 3 seconds was eliminated, since we rarely observed a SST pattern with such a short timespan. We then aligned and averaged 40-sec segments of the global mean (or regionally averaged) spectrogram centering on the detected time points. As control, averaging was also performed based on an identical number of randomly chosen time points, repeated 1,000 times. The average spectrogram segment was then converted to *Z* score by comparing it with the distribution of averaged patterns derived from randomly selected time points.

To investigate the possible relationship between SSTs and eye movements, EOG and EMG signals were also averaged with centering on the detected time points. This was done after taking their absolute values and then under-sampling by averaging within a sliding window (1-sec length, 0.2-sec step) to match the temporal resolution of the spectrograms.

Spatial maps of mid- and high-frequency power changes

For individual electrodes, the mid- and high-frequency BLPs were averaged within a 5-second period preceding the detected time points where the low-frequency activity emerges (corresponding to the period from −5 to 0 second in spectrograms of **Fig 2a** and **2b**). This step results in two spatial profiles (mid- and high-frequency) for each SST event. For a group-level representation, the spatial profiles of individual monkeys (128 channels) were then expanded to group-level profiles (256 channels for sleep and 512 channels for EC condition) using spatial interpolation based on the relative locations of all electrodes. The group-level profiles were then averaged across the SST events to give the final spatial maps of mid- and high-frequency power changes. One sample t-test was performed at each electrode to see whether its power changes are significant ($p < 0.001$, uncorrected).

Results

Characteristics of spontaneous events during sustained sleep

In the sleep recordings (C: n=3; G, n=3), sleep-specific ECoG features such as K-complexes and delta waves typically started to appear after the monkey was left in a dark, quiet room for several minutes. Nevertheless, these electrophysiological events occurred intermittently rather than continuously throughout the recording, consistent with the notion that sleep is not a uniform behavioral state (Halasz et al., 2004; Terzano and Parrino, 2000). Typically, cyclic alternating patterns (CAPs) were observed, characterized by a brief epoch of K-complexes or delta waves (Fig 1b**,** Epoch 3), often followed by a burst of fast oscillations (Epoch 1), alternating with low amplitude ECoG (Epoch 2). CAPs have previously been linked to micro-arousal phenomena and represent a micro-variation in vigilance level during sleep (Halasz et al., 2004; Terzano and Parrino, 2000).

To investigate sequential changes in cortical activity during CAPs, we generated spectrograms by applying time-frequency transformation to the ECoG data (see Methods) and focused on the relative timing of aggregate neuroelectrical activity in specific spectral

frequency bands, the choice of which was based on their established association with behavioral states. We selected a low-frequency delta band (defined as < 4 Hz) because of its association with sleep-specific activity, including slow waves and K-complexes (Steriade, 2006); a mid-frequency alpha-beta (9-21 Hz) band, thought to encompass cortical feedback activity at normal waking consciousness (Buschman and Miller, 2007; van Kerkoerle et al., 2014; von Stein et al., 2000; Yanagawa et al., 2013); and a high-frequency broadband gamma power (42-87 Hz), representing a state of increased cortical activation (Merker, 2013; Sedley and Cunningham, 2013). First, we noticed that signal variations occurred simultaneously over many channels (Fig 1b). In fact, the global mean power variation accounted for a high proportion of the signal variance across channels (35.27±6.78%, 43.98±10.01%, and 43.09±7.46% for the low-, mid-, and high-frequency power variations respectively, mean ± S.D. of individual channels). Based on this finding, during initial analysis we collapsed the data across channels and computed the channel-averaged spectrograms to investigate neural events affecting large regions of the cerebral hemisphere.

The channel-averaged spectrograms revealed a repetitive, stereotypical pattern of band-specific power changes (Fig 1c), consisting of a low-frequency power increase (Epoch 3), *preceded* by both a sudden decline in mid-frequency power (Epoch 2) and an increase in high-frequency power. These changes involved most of the electrodes (Fig. 1d, see below for discussion). The observed sequential spectral transitions (termed SSTs from hereon) coincided with CAP segments where slow wave activity (Fig 1b, Epoch 3) emerged from a low activity baseline (Epoch 2). SSTs lasted typically about 10 seconds and reoccurred at intervals of varying duration, with the longer intervals sometimes lasting minutes and displaying sustained mid-frequency activity (Fig 1c).

To further quantify the SST phenomenon, we identified time points at which the low-frequency activity emerged (see Methods for details). We found 955 such onset time points during ~7.2 hours of recording in 6 experiments on 2 monkeys, with an average interval of 25.2±26.1 seconds (Supp Fig 1). We then averaged the 40-sec segments of the spectrogram centered on these time points. Inspection of this average (Fig 2a) confirmed the initial observation: CAPs contain a reproducible SST pattern in which low-frequency increases are preceded by mid-frequency decreases and high-frequency increases. This sequential order was further confirmed with correlation analysis (Fig 2c). Similar results were observed across 6 sleep experiments and across the 2 monkeys tested (see Supp Fig 2). Interestingly, both EMG and EOG signals also showed a sudden drop associated with the mid-frequency power reduction (Supp Fig 3a).

As sleep and wake conditions were poorly controlled, and are, in general, behaviorally heterogeneous, intermittent arousal events may have also occurred during periods defined as wake. This would likely occur more frequently during the eyes-closed (EC) condition compared to the less sleep-conducive eyes-open (EO) condition. Indeed, analysis of the EC data revealed SST patterns qualitatively similar to those observed during sleep, albeit with a somewhat reduced strength; in contrast, the identical analysis under the EO condition did not show the stereotypical SST pattern (Fig 2b). This progressive weakening of the SST going from sleep to EC to EO was confirmed by correlation analysis (Fig 2c) and is consistent with the notion that it is closely related to vigilance level.

Similar transition pattern at the induction of propofol anesthesia

If SSTs indeed characterize arousal transitions, one would expect their reproducible occurrence after administration of anesthetic agents. To investigate this, we examined the electrophysiological activity after administration of propofol, which causes a transition to a brain state that in many ways resembles that of natural, slow-wave sleep (Murphy et al., 2011). Within less than one minute following a bolus injection of propofol (Fig 3, injection at black arrows), the ECoG of the animals became dominated by low-frequency power. However, close inspection of this transition revealed a pattern of spectral changes that showed resemblance to the SST pattern intermittently observed during sleep and eyes-closed wakefulness (Fig 3, periods inside dash boxes): a drop in mid-frequency power was followed by increases in high- and then low-frequency power. This resemblance, which was consistently observed in four experiments on monkeys C and G (Fig 3), reinforces the idea that the observed SST pattern characterizes a transition into a state of low arousal and is consistent with the notion that such changes are precipitated by a combination of decreasing power in mid-frequency and increasing power in high-frequency bands in the cortex.

Spatial aspects of the sequential spectral transition

With the broad coverage of our recording technique, we were able to investigate not only temporal characteristics of SSTs, but also their spatial aspects. As mentioned above, initial inspection of power variation during sustained sleep revealed a strong level of synchrony across electrodes. To further quantify the extent to which the SSTs in the channel-averaged spectrograms reflect activity of individual electrodes, we computed a spatial synchronization index (SSI), defined as the percentage of channels with concurrent power changes larger than 1 standard deviation (increases in low- and high-frequency, decreases in mid-frequency). Large SSI peaks (~0.8-0.9) appeared at the SSTs (Fig 1d), indicating that large-amplitude power modulations occurred synchronously in the majority of the electrodes, and suggesting a widespread cortical involvement of this neural process. In accordance with this notion, the SST pattern was consistently observed in spectrograms averaged regionally instead of globally (Supp Fig 4).

Despite widespread cortical involvement in the SST, there were *quantitative* differences across regions in the amplitude of power modulation, particularly in the mid- and high-frequency ranges (Supp Fig 4). To further analyze this, we mapped the amplitude of the mid- and high-frequency power changes within a 5-second period preceding the emergence of low-frequency activity. The electrode-based analysis again confirmed the widespread involvement of the SSTs by the fact that 84.8% (99.2%) and 71.5% (64.7%) of the electrodes showed significant ($p < 0.001$) mid-frequency (high-frequency) power changes during sleep and EC conditions, respectively (Fig 4), but it further suggested that the magnitude of the power changes showed considerable spatial variation that was distinctly different for the mid- and high-frequency bands. While the largest high-frequency increases were observed at the early sensory regions, the mid-frequency reductions were most substantial at higher-order regions in parietal, occipito-temporal, and lateral frontal cortices (Fig 4). Considering that one of the putative roles of mid-frequency alpha-beta activity is sensory inhibition through feedback control (Bastos et al., 2012; Engel and Fries, 2010; Jensen and Mazaheri, 2010; Klimesch et al., 2007; Palva and Palva, 2007), the timing and

regional dominance of mid- and high-frequency power modulation suggests that the early mid-frequency drops in SSTs may reflect arousal drops that are mediated through a diminution of feedback inhibitory control.

To further support this interpretation, we quantified the level of negative correlation between mid- and high-frequency powers within and across hierarchical visual regions. A stronger cross-areal correlation would indicate the presence of a cross-hierarchy coupling mechanism. For this purpose, we extracted the mid- and high-frequency powers from the visual association area and the primary visual cortex respectively (Fig 5a), and then calculated cross-correlation functions between the two bands for all possible combinations. Indeed, the strongest coupling was found between the mid-frequency power of the high-order visual area and the high-frequency power of the primary visual cortex (Fig 5b, dark green), with the former leading in time as indicated by the observed asymmetry of the correlation function with respect to the temporal origin (t=0).

Discussion

Electrophysiological data from macaque brain were analyzed to study dynamic modulation of cortical activity associated with vigilance changes. Across large cortical areas, characteristic SSTs, consisting of a sequential modulation of frequency-specific activity, were found at arousal transitions during sleep and at the induction of anesthesia. The temporal order of the sequence of events may suggest that the reduction of cortical feedback activity precedes, rather than is caused by, the emergence of slow waves/oscillations.

Mid-frequency activity and feedback processes

Mid-frequency alpha-beta activity has been linked to top-down, feedback processes because of its critical role in goal-directed tasks (Buschman and Miller, 2007; von Stein et al., 2000) and conscious perception (Maier et al., 2008). Directional analyses of information flow, including one on the dataset studied here (Yanagawa et al., 2013), confirmed this linkage (von Stein et al., 2000; Yanagawa et al., 2013), and further support has come from a recent study examining the cross-layer propagation of alpha activity in V1, as well as frequency-specific response to microstimulation at V1 and V4 (van Kerkoerle et al., 2014). In a complementary fashion, our findings lend support to this notion in terms of the coupling between band-limited power signals. It has been hypothesized that the feedback process associated with the alpha-beta activity takes the form of *inhibitory* control over the activity in the sensory cortex (Bastos et al., 2012; Engel and Fries, 2010; Jensen and Mazaheri, 2010; Klimesch et al., 2007; Palva and Palva, 2007). Consistent with this hypothesis, the reduction of mid-frequency power at SSTs is followed by an increase in broadband gamma power (Fig 2c), which is commonly accepted as a sign of cortical activation (Merker, 2013; Sedley and Cunningham, 2013). Further, the mid- and high-frequency modulations dominate quantitatively at the high- and low-order cortices respectively (Fig 4), and their coupling is stronger across the hierarchical regions than within the same area and initiated by mid-frequency changes in the higher-order cortex (Fig 5). A release from inhibitory control may explain not only the increased high-frequency power during the SSTs, but also the larger

evoked responses of sensory cortices during sleep compared with awake (Massimini et al., 2007; Meeren et al., 1998; Ornitz et al., 1967).

The ocular activity (EOG amplitude signal) drop associated with the mid-frequency power reduction (Supp Fig 3) is also consistent with this feedback hypothesis, since the feedback control from the frontal eye field (FEF) is critical for eye movements. In addition, the EOG and EMG signal reductions also overlap largely with the gamma power increase in the SST (Supp Fig 3), which is therefore unlikely the artifact caused either by ocular activity (Jerbi et al., 2009) or muscle activity. The EMG spikes occurred at the late phase of the SST (*seconds* after the onset) and were only associated with a portion of SST events, therefore they are likely the results of arousal changes, rather than the cause of the SST events.

It should be noted that mid-frequency power reductions may also occur during event-related desynchronization, a phenomenon that occurs during sensory processing (Oswal et al., 2013; Pfurtscheller and Lopes da Silva, 1999). However, compared to SSTs, these power reductions are generally shorter, more local in space, and not followed by bouts of low-frequency activity (Supp Fig 5). A possible functional distinction between event-related desynchronization and SSTs is that the former would reflect an *active*, specific top-down control at sustained levels of consciousness rather than a *passive*, widespread loss of such inhibitory control at LOC.

Finally, it is worth noting that the mid-frequency alpha-beta activity that drops at SSTs is probably distinct from alpha rhythms seen during anesthesia (Tinker et al., 1977; Vijayan et al., 2013). While the former resides largely in the posterior brain (Fig 4), the latter dominates the frontal regions. In fact, the increased frontal alpha during anesthesia is often associated with decreased posterior alpha and the phenomenon was thus also named as alpha anteriorization (Tinker et al., 1977; Vijayan et al., 2013). Inspection on our propofol data did reveal an increase in mid-frequency power at frontal electrodes, but this occurred several minutes after the bolus injection of propofol and outside the time window of Fig 3.

Dissociated modulation of mid- and low-frequency activity

While the early reduction of mid-frequency activity appears to counter earlier notions that the emergence of slow oscillations may be causal to a disruption of the cortico-cortical communication typical of feedback activity (Alkire et al., 2008; Lewis et al., 2012), it does not necessarily imply the reverse causality either. The evolution of the SSTs occurs over several seconds, a time scale much longer than that typical of neuronal interactions. Thus, rather than having a causal influence, the reduction of mid-frequency activity may play a facilitatory role; it may create the necessary condition for the entire transition to play out. One possibility is that mid-frequency activity and slow oscillations share the same neuro-anatomical infrastructure, and that this sharing occurs at the level of cortical layers. In fact, it was recently shown that slow oscillations in in-vitro slices, as well as in anesthetized and sleeping animals, are more likely to be initiated when layer V pyramidal neurons are depolarized (Beltramo et al., 2013; Chauvette et al., 2010; Sanchez-Vives and McCormick, 2000). This layer is a part of the infragranular zone where local field potentials (LFPs) of awake animals were found to exhibit relatively stronger alpha-beta activity than in the supragranular zone (Buffalo et al., 2011; Maier et al., 2010). Thus, the quiescence of alpha-

beta activity in the deep cortical layers may be a necessary condition for the generation of sleep-specific oscillations, in analogy of the relationship between low- and mid-frequency powers found in the current study.

The dissociated modulation of wake-representing alpha-beta activity and sleep-representing delta activity is beyond their reciprocal correlation typically observed with macro-level analyses of sleep electroencephalogram (EEG) (Aeschbach and Borbely, 1993; Mann et al., 1993; Uchida et al., 1992; Uchida et al., 1991). The temporal precedence is consistent with the hypothesis that the process of falling sleep is initiated by a withdrawal from the waking state rather than an invasion of the sleeping state. While this hypothesis was originally suggested based on the observation that the duration of sleep onset is correlated with beta power but not delta power (Merica et al., 1991), it recently gained support from studies on the wake- and sleep-promoting neurons at the basal forebrain, hypothalamus, and brainstem. Mutual inhibition between these two groups of neurons provides the conditions for a rapid switching of brain states (Saper et al., 2010; Saper et al., 2005) and cortical activity pattern (Detari et al., 1984; Lee et al., 2005; Sherin et al., 1996; Szymusiak and McGinty, 1986); however, it has remained unclear whether one, if any, of the two systems preferentially initiates the putative switch that effectuates changes in arousal level. Single unit recordings of these subcortical neurons in non-anesthetized mice during the wake-sleep transition recently showed a decrease in discharge rates of wake-promoting neurons that preceded the onset of cortical synchronization, which in turn precedes the firing of sleep-promoting neurons (Takahashi et al., 2010; Takahashi et al., 2009). Therefore, both these subcortical recordings at the neuronal level, as well as the cortical recording at the systems level presented here, suggest a similar dissociation between modulations of wake- and sleep-associated processes. Future studies with concurrent cortical and subcortical recordings would be critical for fully understanding the interaction of wake- and sleep-promoting systems during SSTs, and more importantly, the relative timing between changes in the mid-frequency cortical activity and wake-promoting neurons.

The spectral recovery at the late phase of each SST suggests that SSTs represent a sequential drop and recovery of arousal, rather than an isolated arousal drop. The observation that the rebound of the mid-frequency power at the late phase of the SSTs (Fig 1c) is often associated with EMG spikes (Supp Fig 3b) is consistent with this notion. Further support derives from the observation that “micro-arousal” events are often associated with CAP structures (Halasz et al., 2004). In contrast, the similar transition pattern at the induction of propofol anesthesia actually lacks such rebounding phase of the mid-frequency power (Fig 3), consistent with an isolated, one-directional transition from conscious to unconscious state. In the same vein, it is possible that the early phase of the SST, i.e., the mid-frequency power reduction, represents transition into “micro-sleep” characteristic of low-arousal wakefulness.

One limitation of the current study is that sleep deprivation was used to increase the sleep propensity of monkeys, and this may quantitatively affect cortical dynamics, particularly around state transitions (Dijk et al., 1993). However, since the CAP phenomenon (the time-domain representation of SSTs) has been widely observed without sleep deprivation (Halasz et al., 2004; Terzano and Parrino, 2000), the structure of SSTs likely generalizes to normal

nocturnal sleep. In fact, it is possible that sequential changes of frequency-specific activity are a general phenomenon associated with state transitions, including those not caused by normal sleep or anesthesia. For example, a recent EEG investigation of cataplexy episodes in narcoleptic children observed intermittent theta bursts (2.5–5 Hz) alternating with the mid-frequency alpha oscillations (8–12 Hz), suggesting the presence of an SST-like phenomenon (Vassalli et al., 2013).

Relation to the global signal in resting-state fMRI

The presence of SST patterns during sleep-conducive conditions may shed some light on the global signal fluctuations that characterize fMRI studies of spontaneous brain activity. The strong band-limited power modulation associated with each SST is likely to trigger large, widespread hemodynamic responses that should be reflected in the fMRI signal. This may explain the findings in a previous study of macaque of a positive correlation between locally recorded gamma LFP power and global fMRI signals, a negative correlation with the mid-frequency power, and a reduction in these correlations with opening of the eyes (Scholvinck et al., 2010). Furthermore, the observation that the high-frequency increase at the SSTs is stronger in sensory regions (Fig 4) is consistent with fMRI studies that found a predominance of sensory activity at brief instances of global cortical activation (Liu and Duyn, 2013a), given the established relationship between fMRI signal and cortical gamma-band activity (Logothetis et al., 2001; Scholvinck et al., 2010).

The notion that SSTs may underlie some of the spontaneous fMRI signal fluctuations is further supported by recent human studies reporting that fMRI signal fluctuations, like SSTs, are strongest during conditions of low vigilance. Fluctuation amplitude and correlations of fMRI signals increased globally not only from wakefulness to light sleep (Fukunaga et al., 2006; Horovitz et al., 2008; Larson-Prior et al., 2009; Olbrich et al., 2009), but also from EO to EC conditions (Bianciardi et al., 2009; Jao et al., 2013; Wong et al., 2013). Most interestingly, the increases in vigilance induced by ingestion of caffeine effectively reduced the amplitude of global signal (Wong et al., 2013), whereas the opposite effects were evident for administration of midazolam (Greicius et al., 2008; Kiviniemi et al., 2005) and zolpidem (Licata et al., 2013), the hypnotic drugs that are known to induce light sedation and drowsiness. Such a relationship is possibly mediated by the appearance of SSTs in states of low vigilance. This is also consistent with observations of activity with event-like characteristics in recent fMRI studies (Liu et al., 2013; Liu and Duyn, 2013b; Petridou et al., 2013; Tagliazucchi et al., 2012).

In summary, the results presented here suggest that in the absence of overt behavior, the brain experiences fluctuations in arousal that are characterized by a reproducible sequence of electrophysiological changes, in which cortical activity typically observed during the wake condition ceases prior to increases in activity commonly associated with sleep. Similar sequence of events was also observed at LOC induced by propofol anesthesia. These results support earlier findings in neuronal populations of sleep and wake promoting systems in the basal forebrain and brainstem of mice (Takahashi et al., 2010; Takahashi et al., 2009), and are consistent with the notion that decreases in the activity of the wake promoting system

facilitate the initiation of arousal drops. A possible mechanism for this facilitation is the passive release of inhibition associated with cross-areal feedback activity.

Supplementary Material

Refer to Web version on PubMed Central for supplementary material.

Acknowledgements

This research was supported (in part) by the Intramural Research Program of the National Institutes of Health, National Institute of Neurological Disorders and Stroke. The authors thank Dr. Picchioni for helpful discussion.

References

Aeschbach D, Borbely AA. All-night dynamics of the human sleep EEG. Journal of sleep research. 1993; 2:70–81. [PubMed: 10607074]

Alkire MT, Hudetz AG, Tononi G. Consciousness and anesthesia. Science. 2008; 322:876–880. [PubMed: 18988836]

Bastos AM, Usrey WM, Adams RA, Mangun GR, Fries P, Friston KJ. Canonical microcircuits for predictive coding. Neuron. 2012; 76:695–711. [PubMed: 23177956]

Beltramo R, D'Urso G, Dal Maschio M, Farisello P, Bovetti S, Clovis Y, Lassi G, Tucci V, De Pietri Tonelli D, Fellin T. Layer-specific excitatory circuits differentially control recurrent network dynamics in the neocortex. Nature neuroscience. 2013; 16:227–234.

Bianciardi M, Fukunaga M, van Gelderen P, Horovitz SG, de Zwart JA, Duyn JH. Modulation of spontaneous fMRI activity in human visual cortex by behavioral state. NeuroImage. 2009; 45:160–168. [PubMed: 19028588]

Boly M, Moran R, Murphy M, Boveroux P, Bruno MA, Noirhomme Q, Ledoux D, Bonhomme V, Brichant JF, Tononi G, Laureys S, Friston K. Connectivity changes underlying spectral EEG changes during propofol-induced loss of consciousness. The Journal of neuroscience: the official journal of the Society for Neuroscience. 2012; 32:7082–7090. [PubMed: 22593076]

Buffalo EA, Fries P, Landman R, Buschman TJ, Desimone R. Laminar differences in gamma and alpha coherence in the ventral stream. Proceedings of the National Academy of Sciences of the United States of America. 2011; 108:11262–11267. [PubMed: 21690410]

Buschman TJ, Miller EK. Top-down versus bottom-up control of attention in the prefrontal and posterior parietal cortices. Science. 2007; 315:1860–1862. [PubMed: 17395832]

Chauvette S, Volgushev M, Timofeev I. Origin of active states in local neocortical networks during slow sleep oscillation. Cerebral cortex. 2010; 20:2660–2674. [PubMed: 20200108]

Davis H, Davis PA, Loomis AL, Harvey EN, Hobart G. Changes in Human Brain Potentials during the Onset of Sleep. Science. 1937; 86:448–450. [PubMed: 17838964]

Detari L, Juhasz G, Kukorelli T. Firing properties of cat basal forebrain neurones during sleep-wakefulness cycle. Electroencephalography and clinical neurophysiology. 1984; 58:362–368. [PubMed: 6207005]

Dijk DJ, Hayes B, Czeisler CA. Dynamics of electroencephalographic sleep spindles and slow wave activity in men: effect of sleep deprivation. Brain research. 1993; 626:190–199. [PubMed: 8281430]

Engel AK, Fries P. Beta-band oscillations--signalling the status quo? Current opinion in neurobiology. 2010; 20:156–165. [PubMed: 20359884]

Fukunaga M, Horovitz SG, van Gelderen P, de Zwart JA, Jansma JM, Ikonomidou VN, Chu R, Deckers RH, Leopold DA, Duyn JH. Large-amplitude, spatially correlated fluctuations in BOLD fMRI signals during extended rest and early sleep stages. Magnetic resonance imaging. 2006; 24:979–992. [PubMed: 16997067]

Greicius MD, Kiviniemi V, Tervonen O, Vainionpaa V, Alahuhta S, Reiss AL, Menon V. Persistent default-mode network connectivity during light sedation. Human brain mapping. 2008; 29:839–847. [PubMed: 18219620]

Halasz P, Terzano M, Parrino L, Bodizs R. The nature of arousal in sleep. Journal of sleep research. 2004; 13:1–23. [PubMed: 14996030]

Horovitz SG, Fukunaga M, de Zwart JA, van Gelderen P, Fulton SC, Balkin TJ, Duyn JH. Low frequency BOLD fluctuations during resting wakefulness and light sleep: a simultaneous EEG-fMRI study. Hum Brain Mapp. 2008; 29:671–682. [PubMed: 17598166]

Imas OA, Ropella KM, Ward BD, Wood JD, Hudetz AG. Volatile anesthetics disrupt frontal-posterior recurrent information transfer at gamma frequencies in rat. Neuroscience letters. 2005; 387:145–150. [PubMed: 16019145]

Jao T, Vertes PE, Alexander-Bloch AF, Tang IN, Yu YC, Chen JH, Bullmore ET. Volitional eyes opening perturbs brain dynamics and functional connectivity regardless of light input. NeuroImage. 2013; 69:21–34. [PubMed: 23266698]

Jensen O, Mazaheri A. Shaping functional architecture by oscillatory alpha activity: gating by inhibition. Frontiers in human neuroscience. 2010; 4:186. [PubMed: 21119777]

Jerbi K, Freyermuth S, Dalal S, Kahane P, Bertrand O, Berthoz A, Lachaux JP. Saccade related gamma-band activity in intracerebral EEG: dissociating neural from ocular muscle activity. Brain topography. 2009; 22:18–23. [PubMed: 19234780]

Jordan D, Ilg R, Riedl V, Schorer A, Grimberg S, Neufang S, Omerovic A, Berger S, Untergehrer G, Preibisch C, Schulz E, Schuster T, Schroter M, Spoormaker V, Zimmer C, Hemmer B, Wohlschlager A, Kochs EF, Schneider G. Simultaneous electroencephalographic and functional magnetic resonance imaging indicate impaired cortical top-down processing in association with anesthetic-induced unconsciousness. Anesthesiology. 2013; 119:1031–1042. [PubMed: 23969561]

Kiviniemi VJ, Haanpaa H, Kantola JH, Jauhiainen J, Vainionpaa V, Alahuhta S, Tervonen O. Midazolam sedation increases fluctuation and synchrony of the resting brain BOLD signal. Magnetic resonance imaging. 2005; 23:531–537. [PubMed: 15919598]

Klimesch W, Sauseng P, Hanslmayr S. EEG alpha oscillations: the inhibition-timing hypothesis. Brain research reviews. 2007; 53:63–88. [PubMed: 16887192]

Ku SW, Lee U, Noh GJ, Jun IG, Mashour GA. Preferential inhibition of frontal-to-parietal feedback connectivity is a neurophysiologic correlate of general anesthesia in surgical patients. PloS one. 2011; 6:e25155. [PubMed: 21998638]

Larson-Prior LJ, Zempel JM, Nolan TS, Prior FW, Snyder AZ, Raichle ME. Cortical network functional connectivity in the descent to sleep. Proceedings of the National Academy of Sciences of the United States of America. 2009; 106:4489–4494. [PubMed: 19255447]

Lee MG, Hassani OK, Alonso A, Jones BE. Cholinergic basal forebrain neurons burst with theta during waking and paradoxical sleep. The Journal of neuroscience: the official journal of the Society for Neuroscience. 2005; 25:4365–4369. [PubMed: 15858062]

Lee U, Ku S, Noh G, Baek S, Choi B, Mashour GA. Disruption of frontal-parietal communication by ketamine, propofol, and sevoflurane. Anesthesiology. 2013; 118:1264–1275. [PubMed: 23695090]

Lewis LD, Weiner VS, Mukamel EA, Donoghue JA, Eskandar EN, Madsen JR, Anderson WS, Hochberg LR, Cash SS, Brown EN, Purdon PL. Rapid fragmentation of neuronal networks at the onset of propofol-induced unconsciousness. Proceedings of the National Academy of Sciences of the United States of America. 2012; 109:E3377–3386. [PubMed: 23129622]

Licata SC, Nickerson LD, Lowen SB, Trksak GH, Maclean RR, Lukas SE. The hypnotic zolpidem increases the synchrony of BOLD signal fluctuations in widespread brain networks during a resting paradigm. NeuroImage. 2013; 70:211–222. [PubMed: 23296183]

Liu X, Chang C, Duyn JH. Decomposition of spontaneous brain activity into distinct fMRI co-activation patterns. Frontiers in systems neuroscience. 2013:7. [PubMed: 23596400]

Liu, X.; Duyn, JH. Resting-State fMRI Signal Anti-Correlation Exists in Absence of Global Signal Regression; In proceedings of 21st ISMRM Annual Meeting; Salt Lake City, Utah, USA. 2013a; p. 2251

Liu X, Duyn JH. Time-varying functional network information extracted from brief instances of spontaneous brain activity. Proceedings of the National Academy of Sciences of the United States of America. 2013b; 110:4392–4397. [PubMed: 23440216]

Liu X, Yanagawa T, Leopold DA, Fujii N, Duyn JH. Robust Long-Range Coordination of Spontaneous Neural Activity in Waking, Sleep and Anesthesia. Cerebral cortex. 2014

Logothetis NK, Pauls J, Augath M, Trinath T, Oeltermann A. Neurophysiological investigation of the basis of the fMRI signal. Nature. 2001; 412:150–157. [PubMed: 11449264]

Magoun HW. An ascending reticular activating system in the brain stem. Ama Archives of Neurology and Psychiatry. 1952; 67:145–154.

Maier A, Adams GK, Aura C, Leopold DA. Distinct superficial and deep laminar domains of activity in the visual cortex during rest and stimulation. Frontiers in systems neuroscience. 2010:4.

Maier A, Wilke M, Aura C, Zhu C, Ye FQ, Leopold DA. Divergence of fMRI and neural signals in V1 during perceptual suppression in the awake monkey. Nature neuroscience. 2008; 11:1193–1200.

Mann K, Backer P, Roschke J. Dynamical properties of the sleep EEG in different frequency bands. The International journal of neuroscience. 1993; 73:161–169. [PubMed: 8169051]

Massimini M, Ferrarelli F, Esser SK, Riedner BA, Huber R, Murphy M, Peterson MJ, Tononi G. Triggering sleep slow waves by transcranial magnetic stimulation. Proceedings of the National Academy of Sciences of the United States of America. 2007; 104:8496–8501. [PubMed: 17483481]

Meeren HK, Van Luijtelaar EL, Coenen AM. Cortical and thalamic visual evoked potentials during sleep-wake states and spike-wave discharges in the rat. Electroencephalography and clinical neurophysiology. 1998; 108:306–319. [PubMed: 9607520]

Merica, H.; Fortune, RD.; Gaillard, JM. Phasic events and dynamic organization of sleep. Vol. 7. Raven Press; New York: 1991. Hemispheric temporal organization during the onset of sleep in normal subjects; p. 73-84.

Merker B. Cortical gamma oscillations: the functional key is activation, not cognition. Neuroscience and biobehavioral reviews. 2013; 37:401–417. [PubMed: 23333264]

Mitra, P.; Bokil, H. Observed Brain Dynamics. Oxford University Press; New York: 2008.

Moruzzi G, Magoun HW. Brain stem reticular formation and activation of the EEG. Electroencephalography and clinical neurophysiology. 1949; 1:455–473. [PubMed: 18421835]

Murphy M, Bruno MA, Riedner BA, Boveroux P, Noirhomme Q, Landsness EC, Brichant JF, Phillips C, Massimini M, Laureys S, Tononi G, Boly M. Propofol anesthesia and sleep: a high-density EEG study. Sleep. 2011; 34:283–291A. [PubMed: 21358845]

Nagasaka Y, Shimoda K, Fujii N. Multidimensional recording (MDR) and data sharing: an ecological open research and educational platform for neuroscience. PloS one. 2011; 6:e22561. [PubMed: 21811633]

Olbrich S, Mulert C, Karch S, Trenner M, Leicht G, Pogarell O, Hegerl U. EEG-vigilance and BOLD effect during simultaneous EEG/fMRI measurement. NeuroImage. 2009; 45:319–332. [PubMed: 19110062]

Ornitz EM, Ritvo ER, Carr EM, La Franchi S, Walter RD. The effect of sleep onset on the auditory averaged evoked response. Electroencephalography and clinical neurophysiology. 1967; 23:335–341. [PubMed: 4167765]

Oswal A, Brown P, Litvak V. Movement related dynamics of subthalmo-cortical alpha connectivity in Parkinson's disease. NeuroImage. 2013; 70:132–142. [PubMed: 23277109]

Palva S, Palva JM. New vistas for alpha-frequency band oscillations. Trends in neurosciences. 2007; 30:150–158. [PubMed: 17307258]

Petridou N, Gaudes CC, Dryden IL, Francis ST, Gowland PA. Periods of rest in fMRI contain individual spontaneous events which are related to slowly fluctuating spontaneous activity. Human brain mapping. 2013; 34:1319–1329. [PubMed: 22331588]

Pfurtscheller G, Lopes da Silva FH. Event-related EEG/MEG synchronization and desynchronization: basic principles. Clinical neurophysiology: official journal of the International Federation of Clinical Neurophysiology. 1999; 110:1842–1857. [PubMed: 10576479]

Sanchez-Vives MV, McCormick DA. Cellular and network mechanisms of rhythmic recurrent activity in neocortex. Nature neuroscience. 2000; 3:1027–1034.

Saper CB, Fuller PM, Pedersen NP, Lu J, Scammell TE. Sleep state switching. Neuron. 2010; 68:1023–1042. [PubMed: 21172606]

Saper CB, Scammell TE, Lu J. Hypothalamic regulation of sleep and circadian rhythms. Nature. 2005; 437:1257–1263. [PubMed: 16251950]

Scholvinck ML, Maier A, Ye FQ, Duyn JH, Leopold DA. Neural basis of global resting-state fMRI activity. Proceedings of the National Academy of Sciences of the United States of America. 2010; 107:10238–10243. [PubMed: 20439733]

Sedley W, Cunningham MO. Do cortical gamma oscillations promote or suppress perception? An under-asked question with an over-assumed answer. Frontiers in human neuroscience. 2013; 7:595. [PubMed: 24065913]

Sherin JE, Shiromani PJ, McCarley RW, Saper CB. Activation of ventrolateral preoptic neurons during sleep. Science. 1996; 271:216–219. [PubMed: 8539624]

Steenland HW. Staying awake: top-down systems control of sleep. OA Neuroscience. 2014; 2:1–14.

Steriade M. Grouping of brain rhythms in corticothalamic systems. Neuroscience. 2006; 137:1087–1106. [PubMed: 16343791]

Szymusiak R, McGinty D. Sleep-related neuronal discharge in the basal forebrain of cats. Brain research. 1986; 370:82–92. [PubMed: 3708324]

Tagliazucchi E, Balenzuela P, Fraiman D, Chialvo DR. Criticality in large-scale brain FMRI dynamics unveiled by a novel point process analysis. Frontiers in physiology. 2012; 3:15. [PubMed: 22347863]

Takahashi K, Kayama Y, Lin JS, Sakai K. Locus coeruleus neuronal activity during the sleep-waking cycle in mice. Neuroscience. 2010; 169:1115–1126. [PubMed: 20542093]

Takahashi K, Lin JS, Sakai K. Characterization and mapping of sleep-waking specific neurons in the basal forebrain and preoptic hypothalamus in mice. Neuroscience. 2009; 161:269–292. [PubMed: 19285545]

Terzano MG, Parrino L. Origin and Significance of the Cyclic Alternating Pattern (CAP). REVIEW ARTICLE. Sleep medicine reviews. 2000; 4:101–123. [PubMed: 12531162]

Thomson DJ. Spectrum estimation and harmonic analysis. Proceedings of the IEEE. 1982; 70:1055–1096.

Tinker JH, Sharbrough FW, Michenfelder JD. Anterior shift of the dominant EEG rhytham during anesthesia in the Java monkey: correlation with anesthetic potency. Anesthesiology. 1977; 46:252–259. [PubMed: 402870]

Uchida S, Maloney T, Feinberg I. Beta (20-28 Hz) and delta (0.3-3 Hz) EEGs oscillate reciprocally across NREM and REM sleep. Sleep. 1992; 15:352–358. [PubMed: 1519011]

Uchida S, Maloney T, March JD, Azari R, Feinberg I. Sigma (12-15 Hz) and delta (0.3-3 Hz) EEG oscillate reciprocally within NREM sleep. Brain research bulletin. 1991; 27:93–96. [PubMed: 1933440]

van Kerkoerle T, Self MW, Dagnino B, Gariel-Mathis MA, Poort J, van der Togt C, Roelfsema PR. Alpha and gamma oscillations characterize feedback and feedforward processing in monkey visual cortex. Proceedings of the National Academy of Sciences of the United States of America. 2014; 111:14332–14341. [PubMed: 25205811]

Vassalli A, Dellepiane JM, Emmenegger Y, Jimenez S, Vandi S, Plazzi G, Franken P, Tafti M. Electroencephalogram paroxysmal theta characterizes cataplexy in mice and children. Brain: a journal of neurology. 2013; 136:1592–1608. [PubMed: 23616586]

Vijayan S, Ching S, Purdon PL, Brown EN, Kopell NJ. Thalamocortical mechanisms for the anteriorization of alpha rhythms during propofol-induced unconsciousness. The Journal of neuroscience: the official journal of the Society for Neuroscience. 2013; 33:11070–11075. [PubMed: 23825412]

von Stein A, Chiang C, Konig P. Top-down processing mediated by interareal synchronization. Proceedings of the National Academy of Sciences of the United States of America. 2000; 97:14748–14753. [PubMed: 11121074]

Wong CW, Olafsson V, Tal O, Liu TT. The amplitude of the resting-state fMRI global signal is related to EEG vigilance measures. NeuroImage. 2013; 83:983–990. [PubMed: 23899724]

Yanagawa T, Chao ZC, Hasegawa N, Fujii N. Large-scale information flow in conscious and unconscious states: an ECoG study in monkeys. PloS one. 2013; 8:e80845. [PubMed: 24260491]

Highlights

- The study identifies a characteristic sequence of spectral power changes
- Similar sequences were observed during sleep and at the induction of anesthesia
- Cross-hierarchy coupling supports alpha-beta activity's role in feedback inhibition
- The reduction of alpha-beta activity precedes the emergence of slow wave activity
- The phenomenon may explain some of global fluctuations in resting-state fMRI

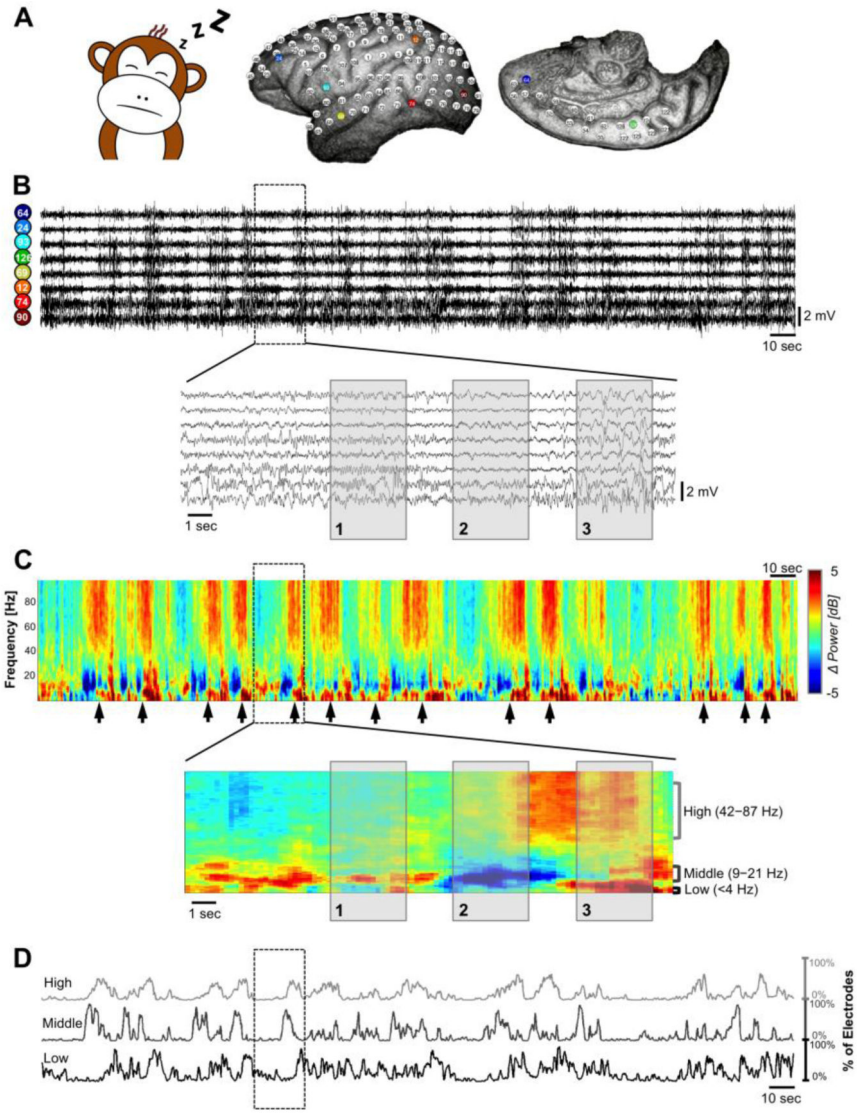

Figure 1.

Sequential spectral transition patterns in ECoG recorded from monkey C during sleep. (a) Spatial topography of 128 electrodes in the monkey C with 6 exemplary ones being marked with colors. (b) A representative, 300 s long ECoG recording from the exemplary electrodes (the upper panel). Inset in lower panel show zoomed-in 20-sec segment. Gray-shaded boxes marked three 3-sec epochs with distinct patterns, which are characterized by alpha-beta oscillation, relatively flat pattern, and high-voltage low-frequency activity, respectively. (c) Global mean spectrogram, averaged over all 128 channels, for the period shown in b. The SST patterns, characterized by sequential modulations in the band-limited power in mid-, high-, and low-frequency bands, are evident even without averaging (the lower panel). (d) Spatial synchronization index (SSI), defined as the fraction of channels showing a power deviation larger than 1 SD, of the three frequency bands for the period shown in b. Deviation is defined as increase in low- and high-frequency powers or decrease in mid-

frequency power. It is evident that power modulations at the SST patterns quickly spread to the majority of the electrodes.

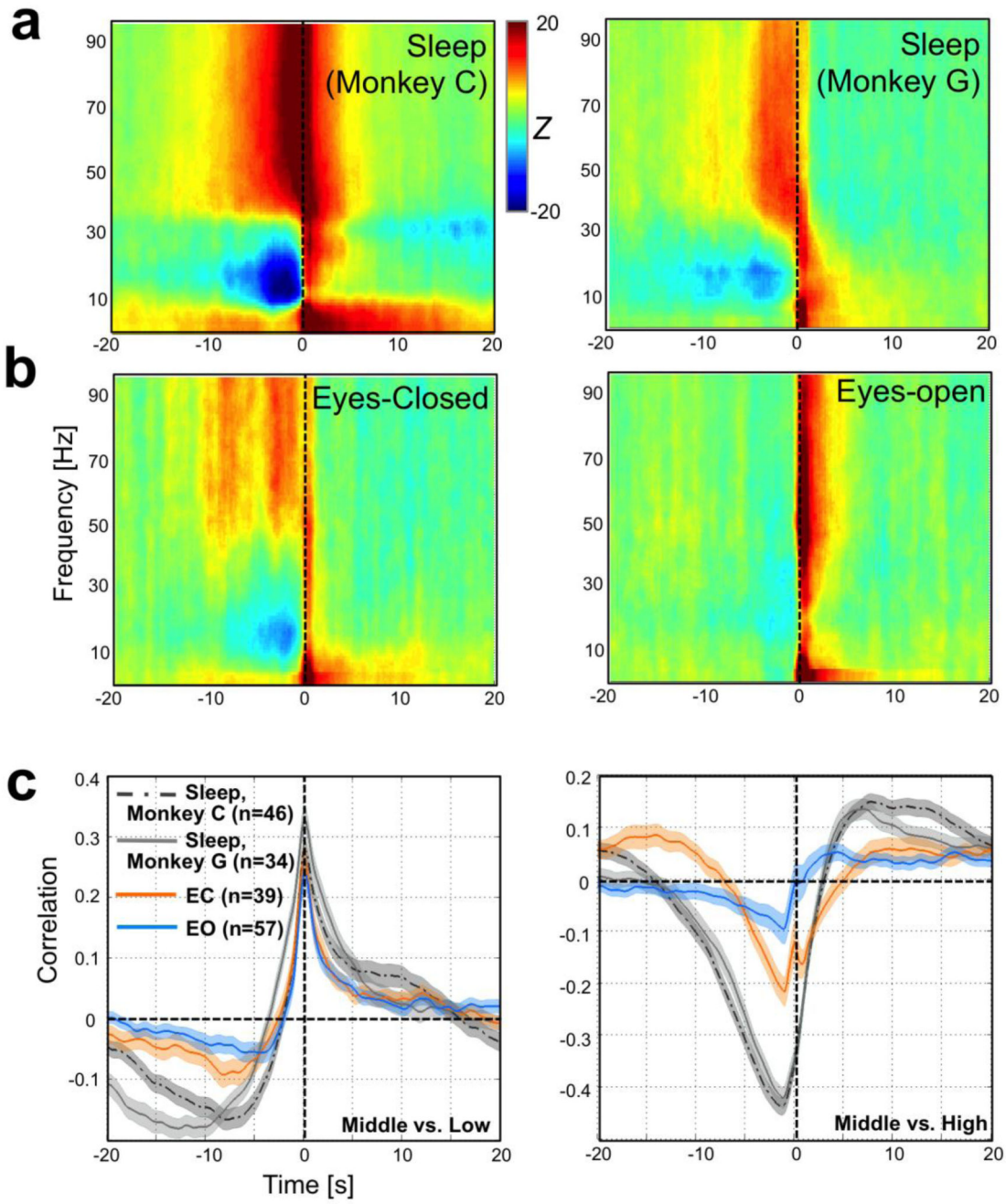

Figure 2.

Average of the SST patterns and cross-correlation functions between different BLPs. (a) Averages of 40-sec segments of the global mean spectrogram in monkey C (left, n=469) and G (right, n=486) around the time points where the low-frequency activity emerged (dash line, t=0); (b) Average patterns under the EC (n=282) and EO (n=629) conditions; (c) Cross-correlations between mid-frequency and low-frequency powers and between mid-frequency and high-frequency powers as a function of their time shifts under various brain states. The cross-correlation functions were calculated for 300-sec sessions and then averaged, and shadows represent areas within 1 standard error of the mean (SEM) across sessions.

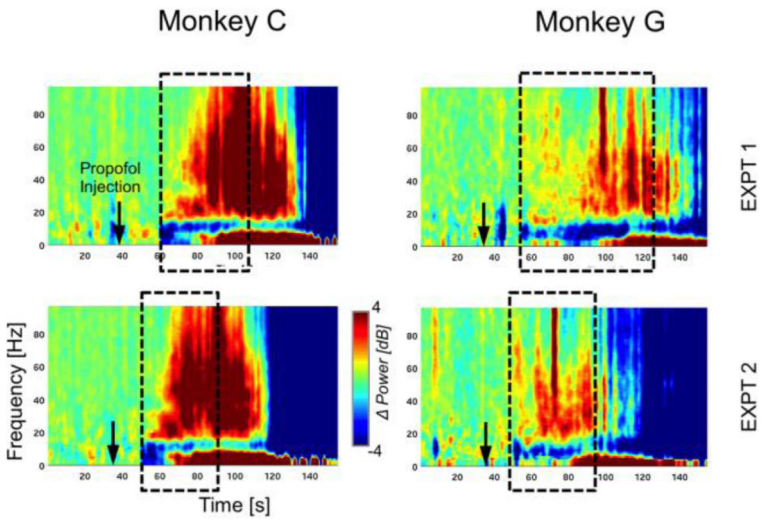

Figure 3.

Sequential spectral transition during the induction of propofol anesthesia. The global mean spectrogram of ECoGs at the beginning of four propofol anesthesia experiments in two monkeys. Black arrows mark the time points where propofol injection started, and dash boxes mark the transition periods showing the sequential spectral transitions. The spectrograms were de-meaned with respect to the periods prior to the injection.

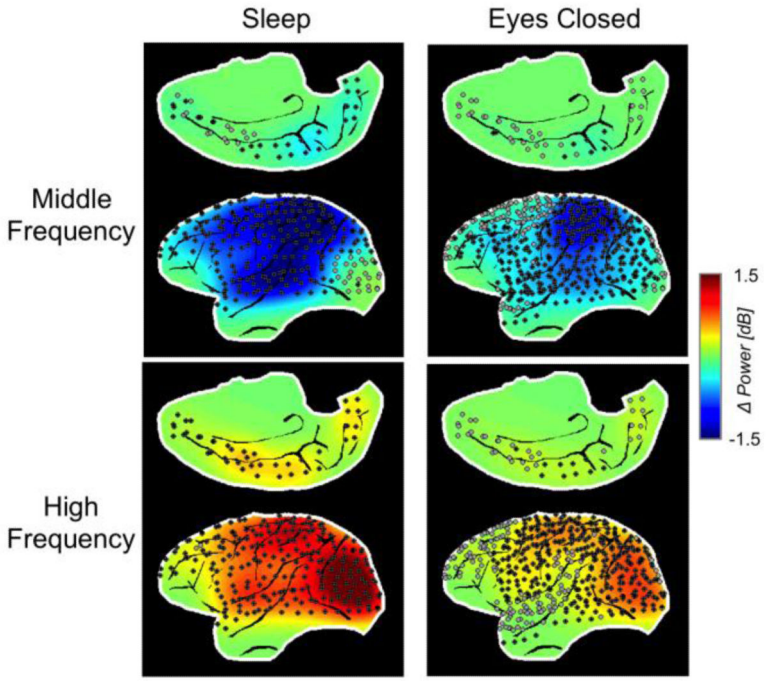

Figure 4.

Spatial distribution of mid- and high-frequency power changes at the sequential spectral transitions. Middle (upper row) and high (lower row) frequency power changes within a 5-second period before the emergence of low frequency activity were analyzed for individual electrodes, averaged across the SST events, and mapped according to electrode locations for the sleep (left) and EC (right) conditions. The electrodes showing significant mid-frequency drops or high-frequency increases ($p < 0.001$, one sample t-test; n = 955, 282 for the sleep and EC conditions, respectively) are marked with asterisks symbols.

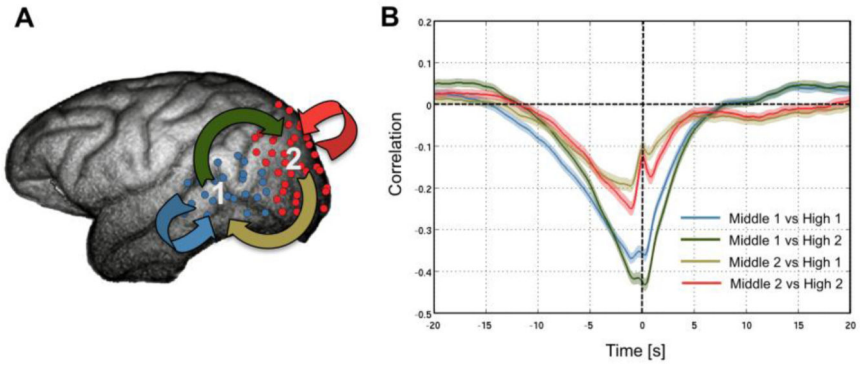

Figure 5.

Within- and cross-areal couplings between the mid- and high-frequency activity during sleep. (a) Mid- and high-frequency powers were extracted from electrodes at the visual association area (area 1, light blue) and the primary visual cortex (area 2, pink red) respectively, which were divided according a network parcellation established previously (Liu et al., 2014). (b) The cross-correlation functions between mid- and high-frequency power were calculated for all possible combinations. Zero-lag coupling was strongest between mid-frequency power in visual association area and high-frequency power in primary visual cortex (dark green), which is 0.070 ± 0.065 lower ($p = 5.5 \times 10^{-15}$, one sample t-test; n = 80 sessions) than the second strongest coupling observed between powers in the visual association area (light blue). The line shadows represent areas within 1 SEM across all 300-sec sessions. The time lag is defined as the mid-frequency relative to the high-frequency power signals.